ACS APPLIED MATERIALS & INTERFACES

Research Article

www.acsami.org

Mechanochemical Approach for Selective Deactivation of External Surface Acidity of ZSM-5 Zeolite Catalyst

Satoshi Inagaki,[†] Koki Sato,[‡] Shunsuke Hayashi,[†] Junichi Tatami,[‡] Yoshihiro Kubota,[†] and Toru Wakihara*[,‡,§]

[†]Division of Materials Science and Chemical Engineering, Yokohama National University, 79-5 Tokiwadai, Hodogaya-ku, Yokohama 240-8501, Japan

[‡]Graduate School of Environmental and Information Sciences, Yokohama National University, 79-7 Tokiwadai, Hodogaya-ku, Yokohama 240-8501, Japan

Supporting Information

ABSTRACT: The acid sites associated with the external surface of zeolite particles are responsible for undesirable consecutive reactions, such as isomerization, alkylation, and oligomerization, resulting in a lower selectivity to a target product; therefore, the selective modification (deactivation) of the external surface of zeolite particles has been an important issue in zeolite science. Here, a new method for surface deactivation of zeolite catalyst was tested via a mechanochemical approach using powder composer. Postsynthetic mechanochemical treatment of ZSM-5 zeolite causes a selective deactivation of catalytically active sites existing only on the external surface, as a potentially useful catalyst for highly selective production of *p*-xylene.

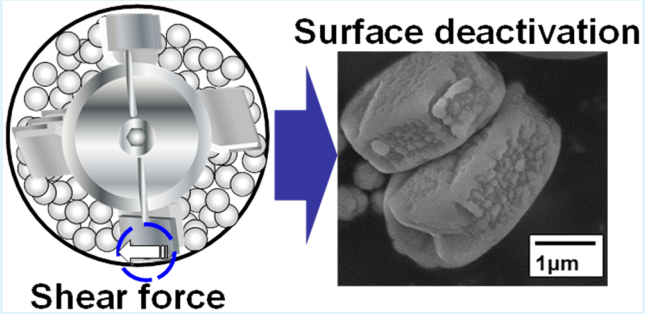

KEYWORDS: *zeolite, powder composer, catalyst, mechanochemical, surface, deactivation*

INTRODUCTION

Zeolites are categorized as crystalline microporous materials composed of tetrahedral metal oxide (e.g., Si and Al) frameworks. Zeolites have multidimensional pore structures with high rigidity (0.2−2.0 nm) and have played important roles in the chemical industry as catalysts, adsorbents, and ion exchangers.[1,2] In many existing applications, such as acid-catalyzed reactions, zeolites are known to exhibit remarkable shape selectivity, owing to their unique pore structure.[3] Alternatively, the acid sites associated with the external surface of zeolite particles are responsible for undesirable consecutive reactions, such as isomerization, alkylation, and oligomerization, resulting in a lower selectivity to a target product. Moreover, such excessive reactions usually lead to catalytic deactivation due to coke deposition on the zeolite particles. To realize higher shape selectivity in the acid-catalyzed reactions, therefore, selective deactivation of the external surface of zeolite particles has been studied by many endeavors, mainly, by taking chemical approaches[4−19] such as impregnation of phosphorus, MgO, and boron,[14,15] chemical vapor deposition,[16,17] chemical liquid deposition,[18,19] and coating with an inactive polycrystalline silicate layer.[4−6] The development of a method for selective modification is still a challenge in zeolite science.

The study presented here focuses on a mechanochemical approach[20] for selective deactivation of the zeolite surface. We employ a powder composite treatment in which fine particles are mechanochemically mixed in a dry mixing process, thus obtaining nanocomposite materials.[21,22] This process has already been applied to the production of ceramic powders and porous ceramics but has yet to be used in the zeolite field.[22] A key distinguishing feature of this process is that particles are brought into contact with one another on an atomic scale by an applied mechanical force, especially a shear force. This paper focuses on the use of shear force for modification of the zeolite surface; that is, the shear force must be effective in deactivating the external surface without destroying the zeolite structure, which is the motivation of the present study. Here we report a new possibility for surface deactivation of zeolite via a mechanochemical route using a powder composer as shown in Figure 1.

This study focuses on ZSM-5 zeolite with MFI topology,[23,24] which consists of two kinds of interconnected 10-ring (10-R) micropores (sinusoidal channel, 0.53 nm × 0.56 nm; straight one, 0.51 nm × 0.55 nm), because this type of zeolite has been most widely industrialized as a solid-acid catalyst in many petrochemical processes, such as fluid catalytic cracking of naphtha and *p*-xylene production from toluene disproportionation and successive xylene isomerization. *p*-Xylene has a

Received: April 17, 2014
Accepted: February 5, 2015
Published: February 5, 2015

DOI: 10.1021/am507982n
ACS Appl. Mater. Interfaces 2015, 7, 4488−4493

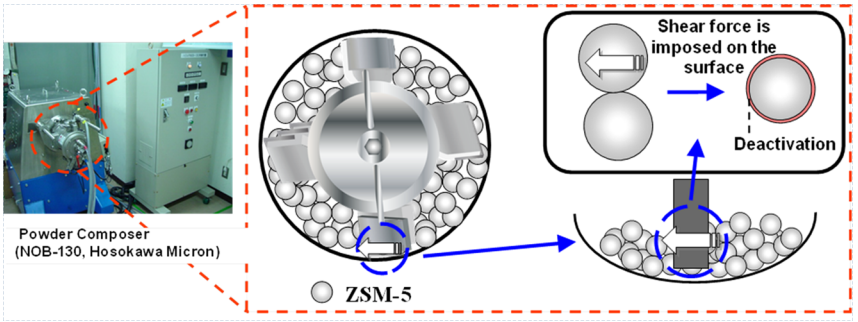

Figure 1. Schematic of mechanochemical treatment of ZSM-5 zeolite.

much higher diffusion coefficient than *o*- and *m*-xylene within the ZSM-5 pores. When the isomerization reaction occurs, *p*-xylene can move along the pores, diffusing out of the zeolite particles promptly. However, secondary isomerization of *p*-xylene into *o*- and *m*-xylene on the external surface reduces the selectivity of *p*-xylene.[7−13] Therefore, we have tried post synthetic mechanochemical treatment of ZSM-5 to realize a selective deactivation of catalytically active sites existing on the external surface, giving a characteristic ZSM-5 zeolite catalyst without external sites. Hence, ZSM-5 zeolite catalyst with higher *p*-xylene selectivity is successfully prepared.

EXPERIMENTAL SECTION

ZSM-5 zeolite (840NHA, MFI-type zeolite, Si/Al = 19.7, cation NH_4^+; Tosoh Co.) was purchased commercially. Typically, 100 g of ZSM-5 zeolite was mechanochemically treated in a powder composer (Nobilta, NOB-130, Hosokawa Micron Co.). Applied power was 3 kW and treatment periods were 3, 10, and 30 min. The morphology and the phases present of the products were characterized by X-ray diffraction (XRD; Multiflex, Rigaku), field emission scanning electron microscopy (FE-SEM; S-5200, Hitachi), and transmission electron microscopy (TEM; 2000FX, JEOL). N_2 adsorption−desorption measurements (Autosorb-1, Quantachrome) and pyridine adsorption Fourier transform infrared (FT-IR) measurements (FT/IR-6100, Jasco) were conducted according to procedures reported in previous works.[25,26]

To examine the external acidity of ZSM-5 zeolite catalysts, 1,3,5-triisopropylbenzene (TIPB) cracking was carried out at 300 °C by employing a pulse technique.[11] A full description of the catalytic reaction tests can be found in Supporting Information (see Figure S1). According to the previous work,[27] toluene alkylation with methanol was carried out under atmospheric pressure in a downflow quartz tube with inner diameter of 8 mm. Prior to the reaction, 100 mg of catalyst was embedded in the quartz tube and preheated at 500 °C for 1 h under helium flow to remove NH_3 and obtain H-ZSM-5. After the temperature was decreased to 400 °C, the feed was switched to a helium stream involving an equimolar mixture of methanol and toluene. Reactants and products in the catalytic reaction were separated on a capillary-type TC-FFAP column (60 m length, 0.25 mm i.d.) and analyzed on a gas chromatograph (GC-2014, Shimadzu) equipped with a flame-ionization detector (see Figure S2, Supporting Information).

RESULTS AND DISCUSSION

Figure 2 shows X-ray diffraction (XRD) patterns of the samples. The Bragg diffractions derived from an MFI structure in the mechanochemically treated samples maintained the same crystallinity as those from the as-received ZSM-5 zeolite. It appears that the applied force, mainly shear force, during mechanochemical treatment is not enough for crystalline ZSM-5 zeolite to be degraded into noncrystalline materials.

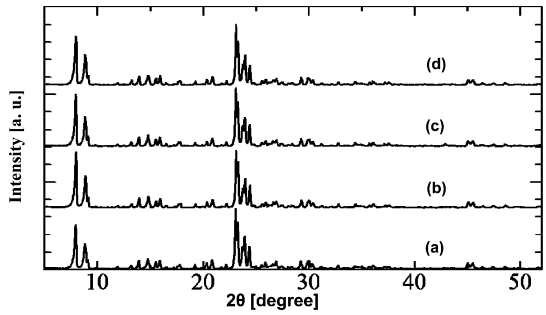

Figure 2. XRD patterns of samples, (a) as received and (b) mechanochemically treated for 3 min, (c) 10 min, and (d) 30 min. All Bragg peaks correspond to an MFI structure.

Brunauer−Emmett−Teller (BET) surface areas, external surface areas, and micropore volumes of the samples are summarized in Table 1. The BET surface areas and micropore volumes of mechanochemically treated samples were almost the same as those of as-received ZSM-5 zeolite, indicating that the bodies of ZSM-5 were almost retained. Alternatively, the external surface area increased from 40 (as-received) to 64 $m^2 \cdot g^{-1}$ (3 min of treatment), and then, it decreased to 46 $m^2 \cdot g^{-1}$ (30 min), indicating that the roughness of the external surface increased and tiny particles are formed in the first few minutes of treatment and then agglomerated again on the external surface of large ZSM-5 particles after 30 min.

Furthermore, significant changes in Si/Al ratios were not seen (data not shown), indicating that the material balance before and after mechanochemical treatment was maintained. It is of note that loss of mass was not confirmed during mechanochemical treatment; that is, the product possessed 99% of the mass of the as-received ZSM-5 zeolite. The high productivity per batch is an advantage of this process. Figure 3 shows typical field-emission scanning electron microscopy (FE-SEM) and transmission electron microscopy (TEM) images of the samples. The as-received zeolite had smooth morphology. However, the ZSM-5 morphology changed drastically after mechanochemical treatment. The as-received zeolite has formed rough surface covered by aggregates composed of fine particles (50−200 nm). This indicates that the fragments formed by the mechanochemical treatment are attached to the surface. After mechanochemical treatment, the morphology of ZSM-5 was rounded (see Figure 3e,f) although the average particle size was almost the same as that for as-received ZSM-5. This indicates that the shear force applied during mechanochemical treatment efficiently modifies only the external surface of the ZSM-5 zeolite, supporting the XRD results. It is also clarified that mechanochemical treatment with higher power for

DOI: 10.1021/am507982n
ACS Appl. Mater. Interfaces 2015, 7, 4488−4493

Table 1. Textural Properties of As-Received and Mechanochemically Treated ZSM-5 Zeolites

catalyst	BET surface area[a] ($m^2 \cdot g^{-1}$)	external surface area[b] ($m^2 \cdot g^{-1}$)	micropore volume[b] ($cm^3 \cdot g^{-1}$)
ZSM-5 (as-received)	434	40	0.173
ZSM-5 (3 kW, 3 min)	438	64	0.170
ZSM-5 (3 kW, 10 min)	425	43	0.169
ZSM-5 (3 kW, 30 min)	434	46	0.163

[a]BET surface area was estimated from the adsorption branch in P/P_0 = 0.01−0.10. [b]External surface area and micropore volume were estimated by the *t*-plot method.

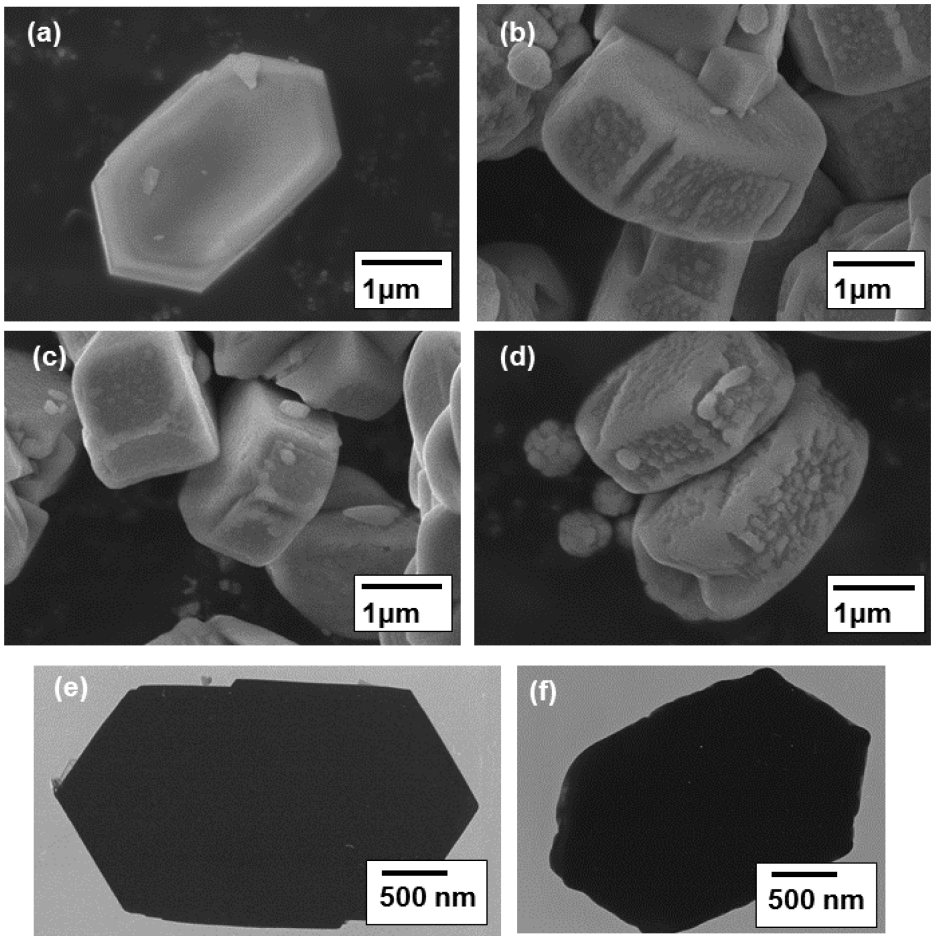

Figure 3. (a−d) FE-SEM images of samples, (a) as received and (b) mechanochemically treated for 3 min, (c) 10 min, and (d) 30 min. (e, f) TEM photographs of samples, (e) as received and (f) mechanochemically treated for 30 min.

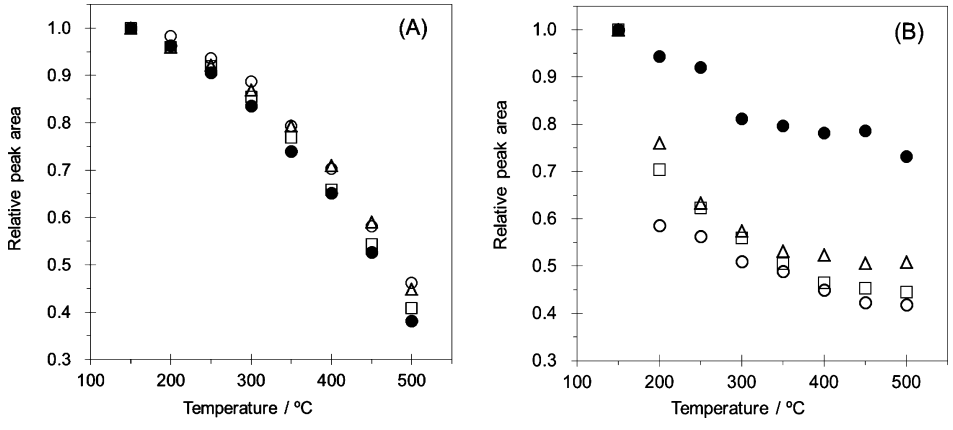

Figure 4. Temperature dependence of peak areas attributed to pyridine adsorbed on (A) Brønsted and (B) Lewis acid sites of ZSM-5, (●) as received and mechanochemically treated for (△) 3 min, (□) 10 min, and (○) 30 min.

DOI: 10.1021/am507982n
ACS Appl. Mater. Interfaces 2015, 7, 4488−4493

a longer period results in a product with a rougher surface and more rounded morphology.

We have attempted to evaluate the change in acidity within ZSM-5 during mechanochemical treatment by means of FT-IR spectroscopy with pyridine adsorption. Typical FT-IR spectra are shown in Supporting Information (Figure S3). The bands at ca. 1545 and ca. 1450 cm^{-1} are attributed to pyridine adsorbed on Brønsted acid sites originated from bridging OH [Si−O(H)−Al] and Lewis acid sites originating from alumina and/or amorphous aluminosilicates, respectively.[26] Figure 4 summarizes the temperature dependence of peak areas attributed to pyridine adsorbed on Brønsted and Lewis acid sites of each ZSM-5 sample. Brønsted acid strength originating from an MFI structure was maintained after mechanochemical treatment. On the other hand, Lewis acid strength of mechanochemically treated ZSM-5 was drastically weakened compared to that of as-received ZSM-5, probably due to transformation of zeolitic structure into amorphous-like aluminosilicates, especially existing on the external surface, via mechanochemical treatment. Unfortunately, until now, a trace amount of the external acid sites within as-received ZSM-5 is not detectable by adsorption of collidine, the size of whichis larger than the 10-R micropores of the MFI framework, via FT-IR measurement.

The catalytic properties of modified ZSM-5 obtained by mechanochemical treatment were evaluated. Catalytic cracking of TIPB on a pulse-type reactor and alkylation of toluene with methanol were performed in a continuous-flow reactor (see Figures S1 and S2, Supporting Information). Catalytic cracking of TIPB occurs only at the external acid sites of ZSM-5 particles, as the size of a TIPB molecule is indeed larger than the 10-R micropores. In contrast, since methanol and toluene molecules are much smaller than TIPB, they can penetrate the 10-R micropores; alkylation of toluene with methanol to xylene can thus evaluate both the external and internal acid sites of ZSM-5 catalysts.

Typical results of catalytic cracking of TIPB are shown in Figure 5. At the first pulse, the as-received ZSM-5 demonstrated high activity in the TIPB cracking reaction (68% TIPB conversion). It should be noted that the mechanochemically treated ZSM-5 samples resulted in less conversion of TIPB than the as-received ZSM-5 (28−38% versus 68%). These results strongly suggest that the external active sites of ZSM-5 have been selectively deactivated by the mechanochemical treatment. When catalyzed by as-received ZSM-5 with a certain number of external acid sites, TIPB conversion gradually decreased with each TIPB pulse as shown in Figure 5, implying that the external acid sites were covered with propylene oligomers and dehydrogenated carboneous species. On the other hand, it is worth noting that, after the second pulse, almost no conversion of TIPB was observed in mechanochemically treated ZSM-5 samples; that is, mechanochemically treated ZSM-5 samples had much lower activity than as-received ZSM-5. This was due to poisoning of the few remaining acid sites on the external surface through coke deposition at the first pulse of TIPB cracking. These results indicate that mechanochemical treatment of ZSM-5 can cause selective deactivation on the external surface; alternatively, the internal surface maintained the acid strength originating from the MFI framework.

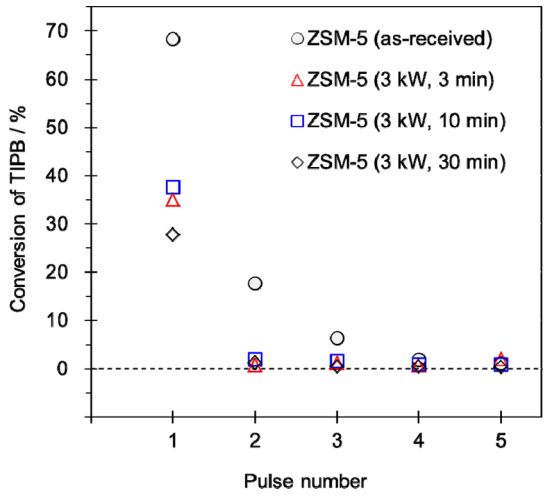

Figure 5. Catalytic behavior in cracking of TIPB in a pulse-type reactor. Reaction conditions: catalyst, 20 mg; temperature, 300 °C; He flow rate, 30 cm^3 (NTP)·min^{-1}; dose amount of TIPB, 0.6 μL.

Toluene alkylation over ZSM-5 catalysts was performed at 400 °C. Catalytic activities of four kinds of ZSM-5 samples and the aromatic product distribution after 65 min of reaction are listed in Table 2. The molar fraction of *p*-xylene relative to all three xylene isomers produced is referred to as the para selectivity. As shown in Table 2, conversions of toluene are nearly the same under these conditions. It is deduced that mechanochemical treatment promotes the formation of a rough surface (and thus increases the area of the external surface) and hence the alkylation of toluene with methanol; however, mechanochemical treatment causes deactivation of the external surface, which in turn lowers the catalytic yield. It appears that nearly the same toluene conversion is determined by the balance between the external surface area and degree of deactivation. It has been shown that as-received ZSM-5 typically has low para selectivity (22.4%) and high selectivity to *m*-xylene (43.2%), indicating that the isomerization of *p*-xylene to other xylene isomers on the external surface is superior.[11] On the other hand, para selectivity of the samples was significantly increased by mechanochemical treatment. The result of high para selectivity can doubtless be explained by selective deactivation of active sites only on the external surface by mechanochemical treatment. It is also of note that the mechanochemically treated layer must be extremely thin and that the pores of ZSM-5 were not plugged, since toluene conversion is nearly the same after mechanochemical treatment. Additionally, the thin layers formed on the external surface of ZSM-5 particles may narrow the mouths of 10-R micropores in the MFI structure, giving higher para selectivity in toluene alkylation. Moreover, when the reaction time passed from 5 to 165 min, para selectivity gradually increased over mechanochemically treated ZSM-5 samples regardless of the stable toluene conversion (25−30%) during this period (see Table S1 in Supporting Information). This behavior is of interest, and we will investigate the details and report elsewhere.

CONCLUSIONS

In summary, a mechanochemical approach was applied for deactivation of acid sites on the external surface of ZSM-5 zeolite. The unique ZSM-5 catalyst had improved *p*-xylene selectivity in the alkylation of toluene with methanol. In this research, we present the mechanochemical treatment of only ZSM-5 zeolite, but further deactivation of acid sites can also be

DOI: 10.1021/am507982n
ACS Appl. Mater. Interfaces 2015, 7, 4488−4493

Table 2. Results of Alkylation of Toluene with Methanol at 400 °C over As-Received and Mechanochemically Treated ZSM-5 Zeolite Catalysts[a]

		product selectivity[b] (%)					
catalyst	conversion of toluene (%)	*p*-xylene	*m*-xylene	*o*-xylene	4-ethyltoluene	1,2,4-trimethylbenzene	material balance[c] (%)
ZSM-5 (as-received)	28.4	22.4	43.2	16.4	8.6	9.2	85.7
ZSM-5 (3 kW, 3 min)	26.6	35.1	36.2	12.6	9.5	6.3	99.5
ZSM-5 (3 kW, 10 min)	26.6	36.0	35.8	12.5	8.9	6.7	91.7
ZSM-5 (3 kW, 30 min)	25.5	41.9	31.7	11.3	8.4	6.5	91.2

[a]Reaction conditions: weight of catalyst, 100 mg; particle size, 500−600 μm; temperature, 400 °C; *P*(toluene), 6.0 kPa; *P*(methanol), 6.0 kPa; He flow rate, 40 cm^3 (NTP)·min^{-1}; time on stream, 65 min. Pretreatment conditions: temperature, 500 °C; time, 60 min; He flow rate, 40 cm^3 (NTP)·min^{-1}. [b]The amount of other aromatic compounds produced in this study was negligible. [c]Material balance was based on the initial amount of toluene.

performed by mechanical mixing with basic materials such as MgO; such works will be reported elsewhere. The mechanochemical treatment proposed in this study is expected to develop as a new methodology for the fabrication of shape-selective catalysts.

■ ASSOCIATED CONTENT

Supporting Information

Three figures, with schematic diagrams of pulse reactor for cracking of TIPB and continuous-flow reactor for alkylation of toluene with methanol and FT-IR spectra of zeolites, and one table listing detailed catalytic results. This material is available free of charge via the Internet at http://pubs.acs.org.

■ AUTHOR INFORMATION

Corresponding Author

* E-mail wakihara@chemsys.t.u-tokyo.ac.jp.

Present Address

[§](T.W.) Department of Chemical System Engineering, The University of Tokyo, 7-3-1 Hongo, Bunkyo-ku, Tokyo 113-8656, Japan.

Notes

The authors declare no competing financial interest.

■ ACKNOWLEDGMENTS

This work was supported by MEXT KAKENHI under Grant 12851437. S.I. thanks Hosokawa Powder Technology Foundation. We thank Professors T. Yokoi and T. Tatsumi at the Tokyo Institute of Technology for making FE-SEM measurements.

■ REFERENCES

(1) Cundy, C. S.; Cox, P. A. The Hydrothermal Synthesis of Zeolites: History and Development from the Earliest Days to the Present Time. *Chem. Rev.* **2003**, *103*, 663−701.

(2) Tosheva, L.; Valtchev, V. P. Nanozeolites: Synthesis, Crystallization Mechanism, and Applications. *Chem. Mater.* **2005**, *17*, 2494−2513.

(3) Fong, Y. Y.; Abdullah, A. Z.; Ahmad, A. L.; Bhatia, S. Development of Functionalized Zeolite Membrane and its Potential Role as Reactor Combined Separator for *para*-Xylene Production from Xylene Isomers. *Chem. Eng. J.* **2008**, *139*, 172−193.

(4) Nishiyama, N.; Miyamoto, M.; Egashira, Y.; Ueyama, K. Zeolite Membrane on Catalyst Particles for Selective Formation of p-Xylene in the Disproportionation of Toluene. *Chem. Commun.* **2001**, 1746−1747.

(5) Miyamoto, M.; Kamei, T.; Nishiyama, N.; Egashira, Y.; Ueyama, K. Single Crystals of ZSM-5/Silicalite Composites. *Adv. Mater.* **2005**, *17*, 1985−1988.

(6) Vu, D. V.; Miyamoto, M.; Nishiyama, N.; Egashira, Y.; Ueyama, K. Morphology Control of Silicalite/HZSM-5 Composite Catalysts for the Formation of *para*-Xylene. *Catal. Lett.* **2009**, *127*, 233−238.

(7) Čejka, J.; Wichterlová, B. Acid-Catalyzed Synthesis of Mono- and Dialkylbenzenes over Zeolites: Active Sites, Zeolite Topology, and Reaction Mechanisms. *Catal. Rev. Sci. Eng.* **2002**, *44*, 375−421.

(8) Sugi, Y.; Kubota, Y.; Komura, K.; Sugiyama, N.; Hayashi, M.; Kim, J. H.; Seo, G. Shape-Selective Alkylation and Related Reactions of Mononuclear Aromatic Hydrocarbons over H-ZSM-5 Zeolites Modified with Lanthanum and Cerium Oxides. *Appl. Catal., A* **2006**, *299*, 157−166.

(9) Mirth, G.; Čejka, J.; Lercher, J. A. Transport and Isomerization of Xylenes over HZSM-5 Zeolites. *J. Catal.* **1993**, *139*, 24−33.

(10) Ding, C.; Wang, X.; Guo, X.; Zhang, S. Characterization and Catalytic Alkylation of Hydrothermally Dealuminated Nanoscale ZSM-5 Zeolite Catalyst. *Catal. Commun.* **2008**, *9*, 487−493.

(11) Inagaki, S.; Shinoda, S.; Kaneko, Y.; Takechi, K.; Komatsu, R.; Tsuboi, Y.; Yamazaki, H.; Kondo, J. N.; Kubota, Y. Facile Fabrication of ZSM-5 Zeolite Catalyst with High Durability to Coke Formation during Catalytic Cracking of Paraffins. *ACS Catal.* **2013**, *3*, 74−78.

(12) Namba, S.; Inaka, A.; Yashima, T. Effect of Selective Removal of Aluminum from External Surfaces of HZSM-5 Zeolite on Shape Selectivity. *Zeolites* **1986**, *6*, 107−110.

(13) Nakasaka, Y.; Tago, T.; Konno, H.; Okabe, A.; Masuda, T. Kinetic Study for Burning Regeneration of Coked MFI-Type Zeolite and Numerical Modeling for Regeneration Process in a Fixed-Bed Reactor. *Chem. Eng. J.* **2012**, *207*, 368−376.

(14) Kaeding, W. W.; Chu, C.; Young, L. B.; Weinstein, B.; Butter, S. A. Selective Alkylation of Toluene with Methanol to Produce para-Xylene. *J. Catal.* **1981**, *67*, 159−174.

(15) Chen, N. Y.; Kaeding, W. W.; Dwyer, F. G. Para-Directed Aromatic Reactions over Shape-Selective Molecular-Sieve Zeolite Catalysts. *J. Am. Chem. Soc.* **1979**, *101*, 6783−6784.

(16) Niwa, M.; Kato, M.; Hattori, T.; Murakami, Y. Fine Control of the Pore-Opening Size of Zeolite ZSM-5 by Chemical Vapor Deposition of Silicon Methoxide. *J. Phys. Chem.* **1986**, *90*, 6233−6237.

(17) Halgeri, A. B.; Das, J. Recent Advances in Selectivation of Zeolites for Para-Disubstituted Aromatics. *Catal. Today* **2002**, *73*, 65−73.

(18) Čejka, J.; Žilková, N.; Wichterlová, B.; Elder-Mirth, G.; Lercher, J. A. Decisive Role of Transport Rate of Products for Zeolite *para*-Selectivity: Effect of Coke Deposition and External Surface Silylation on Activity and Selectivity of HZSM-5 in Alkylation of Toluene. *Zeolites* **1996**, *17*, 265−271.

(19) Breen, J. P.; Burch, R.; Collier, P. J.; Golunski, S. E. Enhanced *para*-Xylene Selectivity in the Toluene Alkylation Reaction at Ultralow Contact Time. *J. Am. Chem. Soc.* **2005**, *127*, 5020−5021.

(20) Abe, H.; Abe, I.; Sato, K.; Naito, M. Dry Powder Processing of Fibrous Fumed Silica Compacts for Thermal Insulation. *J. Am. Ceram. Soc.* **2005**, *88*, 1359−1361.

(21) Hosokawa, M.; Nogi, K.; Naito, M.; Yokoyama, T. *Nanoparticle Technology Handbook*; Elsevier: Oxford, U.K., 2007.

DOI: 10.1021/am507982n
ACS Appl. Mater. Interfaces 2015, 7, 4488−4493

(22) Tatami, J.; Nakano, H.; Wakihara, T.; Komeya, K. Development of Advanced Ceramics by Powder Composite Process. *KONA Powder Part. J.* **2010**, *28*, 227−240.
(23) Baerlocher, Ch.; McCusker, L. B.; Olson, D. H. *Atlas of Zeolite Framework Types*, 6th ed.; Elsevier: Amsterdam, 2007.
(24) Database of Zeolite Structures Home Page. http://www.iza-structure.org/databases/ (accessed December 27, 2014).
(25) Wakihara, T.; Sato, K.; Inagaki, S.; Tatami, J.; Komeya, K.; Meguro, T.; Kubota, Y. Fabrication of Fine Zeolite with Improved Catalytic Properties by Bead Milling and Alkali Treatment. *ACS Appl. Mater. Interfaces* **2010**, *2*, 2715−2718.
(26) Kondo, J. N.; Nishitani, R.; Yoda, E.; Yokoi, T.; Tatsumi, T.; Domen, K. A Comparative IR Characterization of Acidic Sites on HY Zeolite, Silica-Alumina and γ-Alumina using Pyridine and CO probes. *Phys. Chem. Chem. Phys.* **2010**, *12*, 11576−11586.
(27) Inagaki, S.; Kamino, K.; Kikuchi, E.; Matsukata, M. Shape Selectivity of MWW-type Aluminosilicate Zeolites in the Alkylation of Toluene with Methanol. *Appl. Catal., A* **2007**, *318*, 22−27.

DOI: 10.1021/am507982n
ACS Appl. Mater. Interfaces 2015, 7, 4488−4493